Nonstatistical effects in the $^{12}C(^{15}N,\alpha)$ reaction

M. E. Ortiz
Oak Ridge National Laboratory, Oak Ridge, Tennessee 37830
and Instituto de Fisica, Universidad Nacional Autonoma de Mexico, Mexico 20, D.F., Mexico

E. Andrade, M. Cardenas, A. Dacal, and A. Menchaca-Rocha
Instituto de Fisica, Universidad Nacional Autonoma de Mexico, Mexico 20, D.F., Mexico

J. L. C. Ford, Jr., J. Gomez del Campo, R. L. Robinson, and D. Shapira
Oak Ridge National Laboratory, Oak Ridge, Tennessee 37830

E. Aguilera
Instituto Nacional de Investigaciones Nucleares, Mexico D.F., Mexico
(Received 13 March 1980)

States in ^{23}Na were populated using the $^{12}C(^{15}N,\alpha)$ reaction. Excitation functions were measured in the energy range $E_{c.m.}=9.51$–17.33 MeV for 41 states in ^{23}Na from 0 to 12.2 MeV in excitation energy. Angular distributions were measured at selected energies between about 2° and 110° (c.m.). A large number of correlated resonantlike structures with ~400 keV (c.m.) widths were observed in addition to statistical fluctuations in the $^{12}C(^{15}N,\alpha)$ data. Forward peaking of the on-resonant angular distributions appear to be a signature of the excitation of high-spin states in the compound nucleus. Elastic scattering excitation functions measured at backward angles show structures which are not well correlated with the anomalies seen in the reaction channels. The $^{12}C(^{15}N,\alpha)$ data suggest that the resonant portion of the cross sections can be attributed to the population of high-spin levels close to the yrast line of the compound nucleus.

[NUCLEAR REACTIONS $^{12}C(^{15}N,\alpha)$, $E_{^{15}N}=21.4$ to 39.0 MeV, measured $\sigma(E)$ for $\theta_{lab}=7°$; measured $\sigma(\theta)$ for $2\leq\theta\leq110°$ (c.m.) for selected energies; elastic scattering, $E_{^{15}N}=22$ to 31.8 MeV, measured $\sigma(E)$ at 160.2°, 161.4°, 162.6°, 163.8°, and 165° (c.m.); measured $\sigma(\theta)$ for $142\leq\theta\leq170°$ (c.m.) for selected energies, fluctuation, Hauser-Feshbach and single-level analyses.]

I. INTRODUCTION

Nuclear reactions induced by heavy ions with energies of a few MeV per nucleon, in which light ions are emitted, predominantly proceed by compound nucleus formation and decay. The strong absorption of the incident projectiles, the high excitation energy with which the compound nucleus is formed, and the large number of exit channels that are typically open favor an evaporation process as described by the statistical model.[1,2] As a result heavy ions have been extensively employed to investigate statistical processes in light nuclei (see, e.g., Ref. 3). The high angular momentum with which the compound nucleus is formed makes feasible the study of the effects of high spin in both the compound and residual nuclei. High-spin states in *sd* shell nuclei formed by the emission of light ions have been determined by comparison of data with Hauser-Feshbach calculations (see, e.g., Ref. 4). Angular momentum effects also make it possible to extract the moment of inertia of highly excited compound nuclear states from fluctuation analyses of excitation functions.[5]

In contrast to the success of the statistical model in describing many reactions involving light nuclei, it is just in such systems, particularly for $^{12}C+^{12}C$, $^{12}C+^{16}O$, and $^{16}O+^{16}O$, where pronounced resonant effects have been observed in heavy ion reactions.[6] In addition, observation of a direct or semidirect mechanism has been reported for the $^{12}C(^{12}C,\alpha)$ reaction.[7,8] Although resonant and other nonstatistical effects have been clearly identified in systems involving even-even nuclei, the situation is less certain for non-even-even mass nuclei.[9] Resonant strength can be further fractionated due to extra nucleons outside of even-even cores. However, evidence for nonstatistical structure in such systems is also accumulating, as resonant and correlated structure have been reported in the elastic and/or the reaction channels of such systems as $^{10}B+^{14}N$ (Refs. 10 and 11), $^{12}C+^{9}Be$ (Refs. 12 and 13), $^{12}C+^{11}B$ (Ref. 14), $^{12}C+^{13}C$ (Refs. 15–17), $^{12}C+^{14}N$ (Ref. 18), and $^{12}C+^{15}N$ (Ref. 19). Possible direct transfer of eight nucleons has been observed in the $^{12}C(^{10}B,d)$ reaction.[20]

In reality, all heavy ion reactions should display a gradation of effects arising from direct to statistical processes. Those cases where one reac-

tion mechanism dominates are most easily interpreted. However, for many reactions both statistical and nonstatistical effects can be significant and each contains information about the nuclei involved. It is difficult to untangle resonances from statistical fluctuations; they cannot only mask but masquerade as one another. Nevertheless, a careful analysis of such data can often be informative.

In this paper we present $^{12}C(^{15}N,\alpha)$ excitation functions which indicate the presence of a strong and abundant nonstatistical structure. Detailed angular distributions were measured at energies on and off these anomalous peaks. Comparison of the excitation functions and angular distributions with single-level calculations suggest that the origin of the anomalies arises from the excitation of levels close to the yrast line of the compound nucleus. Since the level density of such states is low, a statistical model is inappropriate for levels with high-spin values. Shell-model calculations of the yrast states in ^{27}Al for excitation energies of about 30 MeV and with spin values $\leq \frac{27}{2}^+$ performed by McGrory[21] are consistent with the proposed interpretation that states near the yrast line are being populated in the present experiment. Initial results of this work were reported earlier.[19]

II. EXPERIMENTAL PROCEDURE AND RESULTS

Self-supporting carbon foils (~10 $\mu g/cm^2$) were bombarded with ^{15}N ions accelerated by the ORNL EN tandem. Thirty excitation functions at 7° (lab) were measured in 200 keV intervals for bombarding energies between 21.4 and 39.0 MeV by detecting the emitted α particles at the focal plane of a split-pole spectrograph. Excitation functions for an additional 11 states from 9.5 to 12.2 MeV in ^{23}Na were measured over a more limited range of incident energies. A typical spectrum is shown in Fig. 1. Several of the peaks are labeled by the excitation energies (MeV) in ^{23}Na and spins taken from Refs. 5 and 22–25.

To minimize carbon buildup during irradiation a cold trap was placed between the scattering chamber and the diffusion pump initially used in the experiment. Later the diffusion pump was replaced by a cryopump. During the measurement of the excitation functions the carbon buildup was monitored by recording the total number of α particles detected every 10 μC. Uncertainties in the extracted cross sections were ±10% due to target thickness uncertainty, counting statistics, and carbon buildup.

These measurements, covering a wide interval of incident as well as excitation energies in ^{23}Na, then yield a very large sample (containing over 3000 cross section values) for comparison with the statistical model. Figure 2 displays excitation functions, for states between 0 and 6.04 MeV in

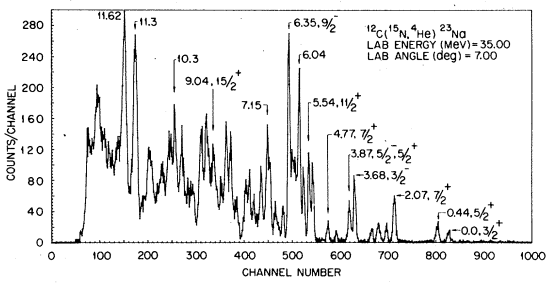

FIG. 1. A $^{12}C(^{15}N,\alpha)$ spectrum measured at a bombarding energy of 35 MeV and a lab angle of 7°.

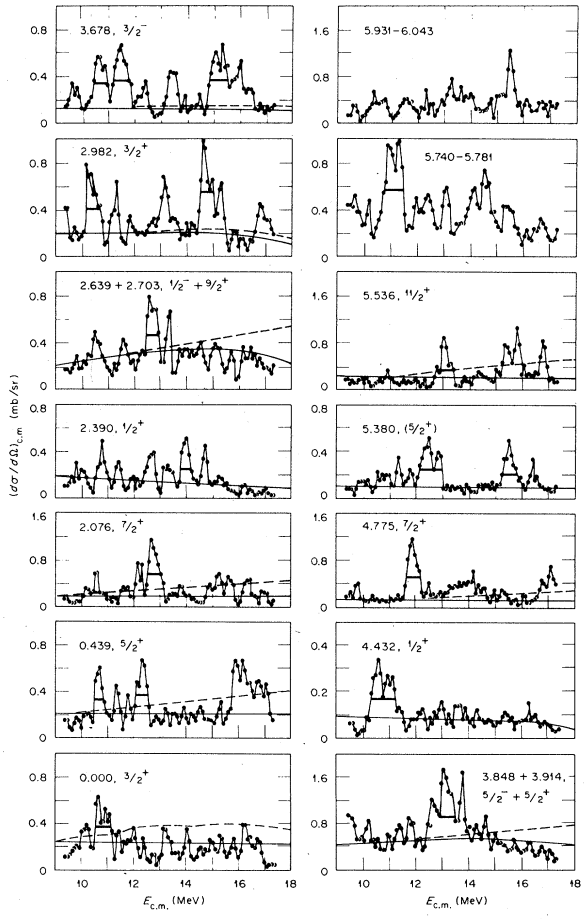

FIG. 2. Excitation functions for states excited in ^{23}Na from 0 to 6.04 MeV. The solid and dashed lines are the results of Hauser-Feshbach calculations discussed in the text. The short heavy lines indicate structures with widths about 2 or 3 times as broad as the coherence width in ^{27}Al.

^{23}Na, which are typical of those measured. As expected, oscillations are observed with widths approximately that of the fluctuation or coherence width (~100–200 keV). Determination of the coherence width by the conventional method of counting the peaks due to the most rapid fluctuations in the data yields a width of ~150 keV for excitation energies between 28 and 33 MeV in ^{27}Al.[26] This value is in reasonable agreement with systematics in this mass region.[27]

However, in addition to the rapid fluctuations observed in the data, and which are expected from the statistical model to be strongest at a forward angle such as 7°, a second underlying structure is also apparent in the excitation functions. A large number of peaks such as those indicated by short horizontal lines are several times as wide as the coherence width. These structures will be discussed in Sec. III A. Despite the observation of resonant-like structures in the excitation functions, the energy averaged cross sections can be compared with Hauser-Feshbach calculations, particularly in energy regions where the structure is not pronounced. Such comparisons with energy averaged excitation functions and angular distributions have been used to suggest high-spin states in ^{23}Na.[28,29] The solid and dashed lines in Fig. 2 correspond to Hauser-Feshbach calculations to be described in Sec. III.

In order to gain further information about the nature of the observed resonant-like structure, detailed angular distributions were measured at selected energies both on and off resonance. These measurements were performed with a position sensitive solid state counter mounted directly in the scattering chamber. A collimator with 14 slits, separated by 1 $\frac{3}{4}$° (c.m.), was used to define the angles. Angular distributions were measured over a range of angles, which in come cases extended from 2° to 110° (c.m.). Figure 3 shows, as an example, distributions measured on and off one of the more prominant peaks observed in the excitation function corresponding to the 2.07-MeV state in ^{23}Na. These two energies are indicated on the portion of the excitation function shown as an insert in the figure. Figure 3 illustrates what appears to be the most characteristic features of the angular distributions. First of all, they are much more strongly forward peaked on resonance than off resonance. Second, the integrated cross section on resonance is not only, as expected, larger than off resonance, but the differential cross section is also larger on resonance at most of the angles measured. This implies that excitation functions measured at various angles will generally also display the bump seen at 28.6 MeV in the 7° excitation function appearing in Fig. 3.

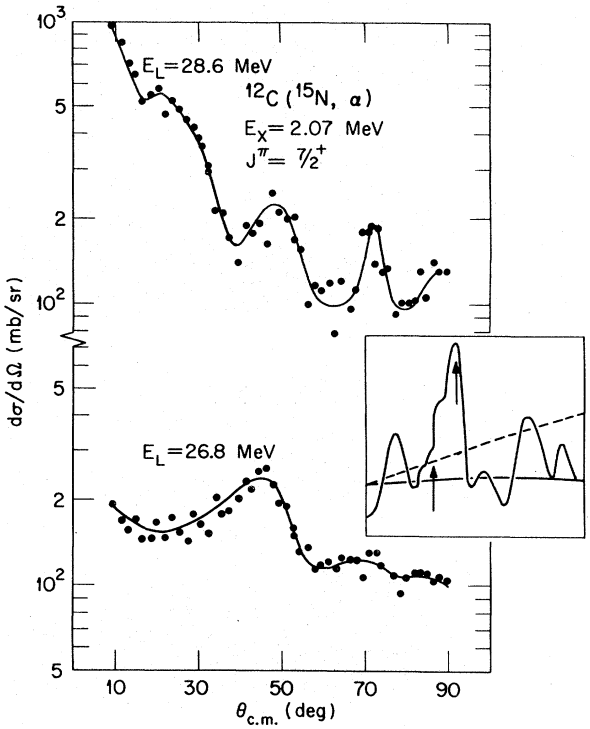

FIG. 3. Angular distributions measured on and off the prominent peak observed at 28.6 MeV in the 7° excitation function for the 2.07-MeV level of ^{23}Na (insert). The solid lines are guides to the eye indicating the forward peaking which occurs on resonance.

The angular distributions and their analysis are further discussed in Sec. III B.

The forward peaking of the angular distributions on resonance as seen in Fig. 3 indicates that the resonant-like effects will be obscured as the reaction angle increases. However, recent elastic and inelastic scattering measurements involving light and *sd* shell nuclei reveal pronounced resonant effects at angles near 180°.[30] Consequently, the back-angle elastic scattering of ^{15}N from ^{12}C was investigated, since it had promise of providing additional information of resonant behavior in this system. The recoiling ^{12}C ions were detected at the spectrograph focal plane at five scattering angles from 5.1 to 9.9° (lab) which correspond to back-angle scattering between 169.8 and 160.2° (c.m.). Excitation functions were measured for bombarding energies between 22 and 31.8 MeV. At isolated energies of interest indicated by the (^{15}N, α) reaction data more detailed angular distributions were measured between 140 and 170° (c.m.). The hybrid counter system employed at the focal plane of the spectrograph is discussed in Ref. 31. The data were measured simultaneously at the five angles by means of a multislit aperture

located at the entrance of the spectrograph. The elastic scattering results appear in Sec. III C.

III. ANALYSES

A. Excitation functions

1. Fluctuation analysis

The presence of intermediate width structure underlying the fine structure in the excitation functions is evident in Fig. 2. An analysis by means of autocorrelation functions can provide information concerning the width of the structure in excitation functions. If the reaction mechanism is purely statistical then the expectation value of the autocorrelation function is given by

$$R(\epsilon)=\frac{\langle\sigma(E)\sigma(E+\epsilon)\rangle_{I_1}}{\langle\sigma(E)\rangle_{I_1}\langle\sigma(E)\rangle_{I_2}}-1\,, \tag{1}$$

where intervals I_1 and I_2 are $(E_1, E_2-\epsilon)$ and $(E_1+\epsilon, E_2)$, respectively, and E_1 and E_2 are the lowest and highest energies under consideration, approaches a Lorentzian with a width at half-maximum of Γ, the average decay width of the compound states, as the energy interval E_2-E_1 increases without limit.[32,33] Figure 4 presents the autocorrelation functions obtained from the excitation functions for the 0, 0.44, 3.84, and 8.45 MeV states in ^{23}Na measured at a laboratory angle of 7°. For comparison are shown autocorrelations functions obtained by Halbert *et al.*[34] for the first two levels populated in the $^{12}C(^{16}O,\alpha)$ reaction. Although there is evidence for nonstatistical contributions to this reaction,[34,35] nevertheless, at the energies of concern here, the $^{12}C(^{16}O,\alpha)$ reaction appears to predominantly proceed by a compound nuclear process.[34,36,37] The $^{12}C(^{16}O,\alpha)$ autocorrelation functions shown in Fig. 4 support this picture, as the widths at half maximum of the curves are ~100–125 keV (Ref. 34) and are close to the expected values of the coherence width.[27] The vertical lines in Fig. 4 labeled Γ and 3Γ represent a width equal to the measured coherence width of 158 keV in ^{27}Al (for E_x = 32 MeV) (Ref. 5) using the peak counting technique and a value three times this width. Clearly the autocorrelation functions for the $^{12}C(^{15}N,\alpha)$ reaction are very different than those for $^{12}C(^{16}O,\alpha)$. The width obtained from the $^{12}C(^{15}N,\alpha)$ autocorrelation functions, 223 ± 118 keV, is not only substantially larger than the extracted coherence widths, but also has a standard deviation 2 to 3 times larger than that expected from a purely statistical ensemble of data. As indicated by the dashed lines in Fig. 4, the autocorrelation functions display a structure resembling two overlapping Lorentzians with widths of about Γ and 3Γ.

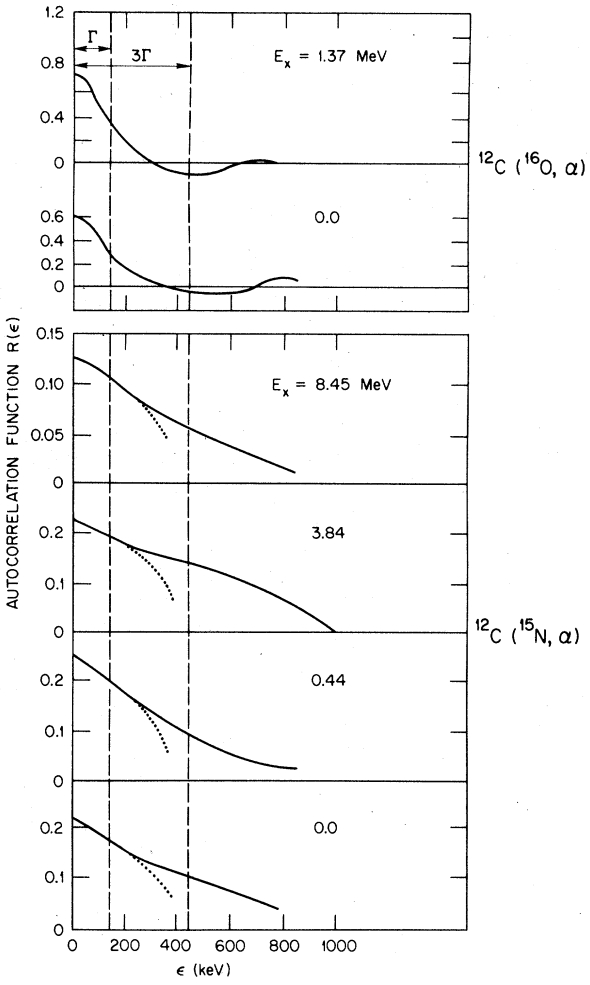

FIG. 4. Comparison of autocorrelation functions for the $^{12}C(^{16}O,\alpha)$ (Ref. 34) and the $^{12}C(^{15}N,\alpha)$ reactions. The dotted and vertical lines indicate how the $^{12}C(^{15}N,\alpha)$ functions appear to be approximated by two Lorentzian curves with different widths.

Further evidence of the width of the structures dominating an excitation function can be obtained by plotting the value of the autocorrelation function $R(\epsilon=0,\Delta)$ determined for an averaging interval Δ, as a function of the averaging interval.[38] This function should increase for values of Δ smaller than the width of structures in the data but begin to flatten out and then remain constant as Δ approaches and then exceeds the width. Figure 5 presents typical results obtained from analyzing the excitation functions. Definite bends begin to appear in the set of curves at Δ values greater than ~2.5 times the coherence width, thus collaborating the structure suggested in Fig. 4.

It is true that the widths obtained from autocorrelation functions often exceed those obtained from the peak counting method (see, e.g., Refs. 26 and 27). This difference is, however, itself indica-

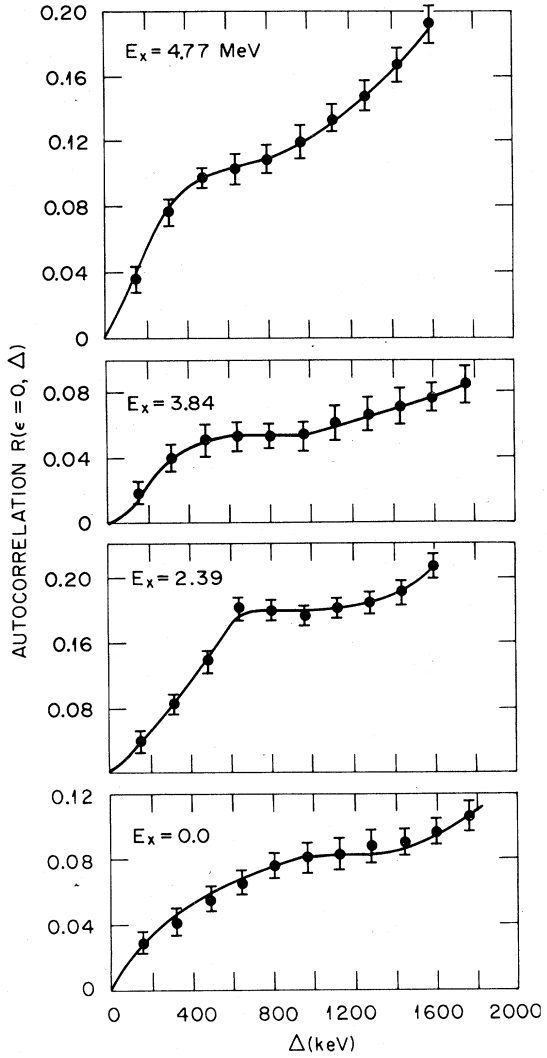

FIG. 5. Autocorrelation functions for $\epsilon = 0$ plotted as a function of the energy interval Δ used to average the data in the excitation functions. The solid lines are merely guides to the data points.

tive of the presence of structure in the excitation functions other than that due to only statistical fluctuations. In a purely statistical ensemble of data the two methods should give identical values for the coherence width (except for the expected statistical uncertainties). But generally widths determined from these two techniques differ by factors between ~1.2 and 1.5. However, the autocorrelation function analyses shown in Fig. 4 and 5 indicate the presence of structures with widths from 2.2 to 3.5 times the coherence width (as do the excitation functions themselves).

2. *Hauser-Feshbach analysis*

In order to emphasize the underlying resonant structure, a running average of the data was performed using an averaging interval Δ equal to about 2.5 times the coherence width. Averaged cross sections for some of the data, such as shown in Fig. 6, were then compared with Hauser-Feshbach calculations.[1,39] The formalism for the cross sections and level-density formulas needed in the computer code HELGA[40] used in these calculations are described in Ref. 41. For example, the total cross section is of the form

$$\sigma_{\alpha',\alpha} = \pi\lambda^2 \sum_{J\pi} \frac{2J+1}{(2I+1)(2i+1)} \frac{\sum_{sl} T^J_{\alpha s l} \sum_{s'l'} T^J_{\alpha' s' l'}}{G(J)}$$

$$= \pi\lambda^2 \sum_J \sigma_J \,, \qquad (2)$$

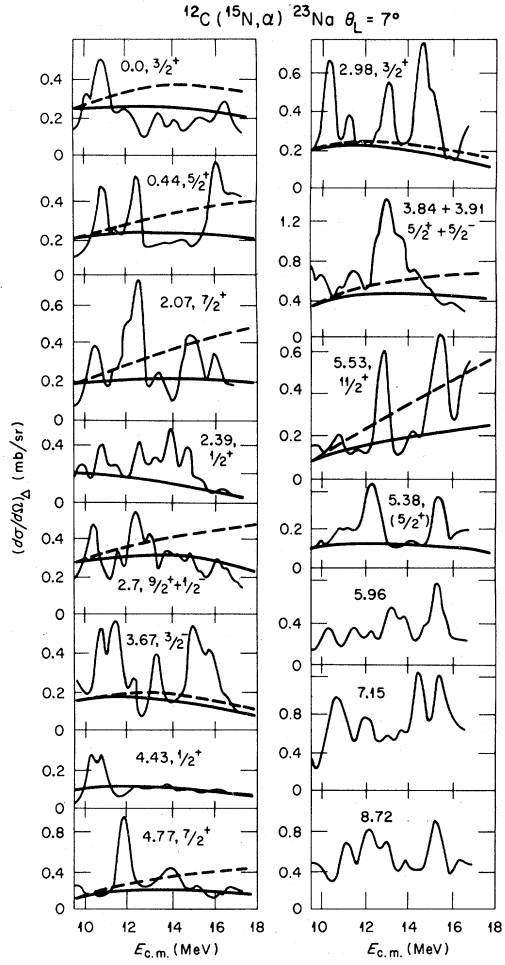

FIG. 6. Excitation functions for the $^{12}C(^{15}N,\alpha)$ reaction averaged over an interval Δ equal to ~2.5 times the coherence width. The results of Hauser-Feshbach calculations without angular momentum cutoff (dashed curves) and with cutoff (solid curves) are indicated for states of known or probable spins.

where unprimed and primed quantities refer to the entrance and exit channels, respectively. Each channel α' has orbital angular momentum l', and channel spin $\vec{s}' = \vec{I}' + \vec{i}'$ leading to a total angular momentum J. The spins I' and i' of the two reaction products are denoted by I and i in the entrance channel. The optical-model transmission coefficients $T^J_{\alpha s l}$ were calculated for each energy of the incoming and outgoing particles by using optical-model parameters included in the input list of the program.

The demoninator $G(J)$ of Eq. (2) includes all decay modes energetically open to the compound nucleus as follows:

$$G(J) = \sum_{\alpha'' l'' s''} \left(\sum_{E_x=0}^{E_c} T^J_{\alpha'' l'' s''} + \sum_{I'' \pi''} \int_{E_c}^{E\max} \rho(\epsilon, I'', \pi'') T^J_{\alpha'' l'' s''} d\epsilon \right), \tag{3}$$

where the double primes refer to all possible exit channels. The sum from $E_x = 0$ to E_c is over known discrete levels, and the integral from E_c to $E_{\max}$ is for continuum states calculated from the level density $\rho(\epsilon, I, \pi)$ and extends from an energy E_c, selected above the last discrete level included in the calculation, up to $E_{\max}$, the highest excitation which is kinematically allowed. The quantity $G(J)$ is a measure of the number of open channels available for the decay of the compound nucleus excited to states with total angular momentum J.

The level density and optical-model parameters employed in the calculations (see Table I) are standard and very similar to those used to successfully fit a variety of statistical reaction data (see, e.g., Refs. 3, 4, 17, 18, 22, 28, 29, 36, 37, and 41). As indicated above in Eq. (2), the cross section can be written as a sum of terms for different values of J, the total angular momentum, extending up to the maximum value permitted by angular momentum conservation. However, there is ample evidence that in many cases the sum over σ_J in Eq. (2) should be terminated at a lower angular momentum value, the critical angular momentum J_c, above which compound nucleus formation is inhibited.[2,50-52] The solid and dashed lines drawn through the averaged excitation functions in Fig. 6 are the results of Hauser-Feshbach calculations with and without the effects of the above angular momentum cutoff. These values for the angular momentum cutoff J_c were obtained by using the sharp cutoff approximation to the fusion cross sections measured by Kovar *et al.*[42] As seen in Fig. 6, the resulting calculations describe the excitation functions of known spin states in energy regions where correlated structure is absent. Such regions occur, for example, above 12 MeV (c.m.) for the 0.0 and 4.43 MeV states, above 13 MeV for the 2.7 MeV doublet and 4.77 MeV level, and between 13 and 15 MeV for the 0.44 MeV state. In general, the Hauser-Feshbach calculations gave reasonable fits to nonresonant regions of the excitation functions or pass through the minima in the resonant structure, and so adequately account for the portion of the observed cross sections due to statistical processes. However, the average cross sections are not predicted by the Hauser-Feshbach calculations [for example, the experimental ratio of the average cross sections for the 2.98 and 0.0 MeV states is about two (see Fig. 6) while those calculated, with or without cutoff, are less than one]. Furthermore, the large peaks observed in the data are frequently 2 and 3 times the average Hauser-Feshbach background and thus are not easily explained on the basis of the statistical model alone.

In addition, many of the peaks for the different particle groups appear to be correlated at various incident energies. For example, in Fig. 7 are some of the 13 or more excitation functions which peak near 10.7 MeV. The shifts in the energies at which the maxima of the peaks occur are small compared with the width of the structures themselves. Figure 8 shows, as another case, some of the approximately 20 excitation functions which peak near 13.2 MeV.

The number of apparent correlations observed is also hard to reconcile with the statistical model. The 41 measured excitation functions contain 216 identified peaks with widths of ~3Γ. If one divides this number of peaks by the total number of bins of this width in the data set in order to estimate the probability p of observing such a peak in an excitation function, then the probability of finding a number r of such peaks in N statistically independent trials or excitation functions is approximated by the binomial distribution

$$P^N_r = \frac{N!}{(N-r)!\,r!}\, p^r (1-p)^{N-r}. \tag{4}$$

Figure 9 compares the predicted and observed probability distributions. The main peak in the distribution of the data is shifted from the calculated value of eight events and there are both more and fewer correlations observed than predicted by the simple binomial distribution. The clustering near zero may be a result of the averaging interval used to smooth the data as well as overlooking smaller structure in the excitation functions. However, Fig. 9 indicates that there are more correlations present than expected from a random set of data.

TABLE I. Level density and optical-model parameters for the $^{15}N + ^{12}C$ reaction.

	$^{23}Na + \alpha$	$^{26}Mg + p$	$^{26}Al + n$	$^{25}Mg + d$	$^{24}Mg + t$	$^{22}Ne + {}^{5}Li$	$^{15}N + ^{12}C$
a	3.06[a]	3.10[a]	3.46[a]	3.70[b]	3.58[b]	2.93[a]	
Δ[c]	2.67	4.26	0.0	2.46	5.13	6.0	
E_c (MeV)	14.7	6.9	3.75	4.4	10.0	7.8	4.5
No. of discrete levels	255	20	23	14	28	30	2
V (MeV)	51.20[d]	$56.99 - 0.55E$[e]	$47.01 - 0.26E$[e]	$89.3 - 0.22E$[e]	166.1[f]	$7.5 + 0.4E_{\text{c.m.}}$[g]	14.00[h]
$R_0 = r_0 A^{1/3}$fm	4.86[d]	3.70[e]	3.86[e]	3.36[c]	3.10[f]	$1.35(A_1^{1/3} + A_2^{1/3})$[g]	$1.35(A_1^{1/3} + A_2^{1/3})$[h]
a_0(fm)	0.57[d]	0.65[e]	0.66[e]	0.81[e]	0.83[f]	0.45[g]	0.35[h]
W (MeV)	20.50[d]	13.50[e]	$9.52 - 0.053E$[e]	$14.4 + 0.24E$[e]	19.30[f]	$0.4 + 0.125E_{\text{c.m.}}$[g]	$0.4 + 0.1E_{\text{c.m.}}$[h]
$R_i = r_i A^{1/3}$fm	4.86[d]	4.29[e]	3.72[e]	3.92[e]	4.98[f]	$1.35(A_1^{1/3} + A_2^{1/3})$[g]	$1.35(A_1^{1/3} + A_2^{1/3})$[h]
a_i(fm)	0.57[d]	0.47[e]	0.48[e]	0.68[e]	0.87[f]	0.45[g]	0.35[h]
R_{Coul}(fm)	4.25[d]	3.70[e]		3.36[e]	3.10[f]	$1.35(A_1^{1/3} + A_2^{1/3})$[g]	$1.35(A_1^{1/3} + A_2^{1/3})$[h]

[a] Values of a are $A/7.5$ for α and n channels, $A/8.4$ for p channel, and $A/6.4$ for ^{5}Li channel.
[b] Values from Ref. 43.
[c] Values from Ref. 44.
[d] Values from Ref. 45.
[e] Values from Ref. 46.
[f] Values from Ref. 47.
[g] Values from Ref. 48.
[h] Values from Ref. 49.

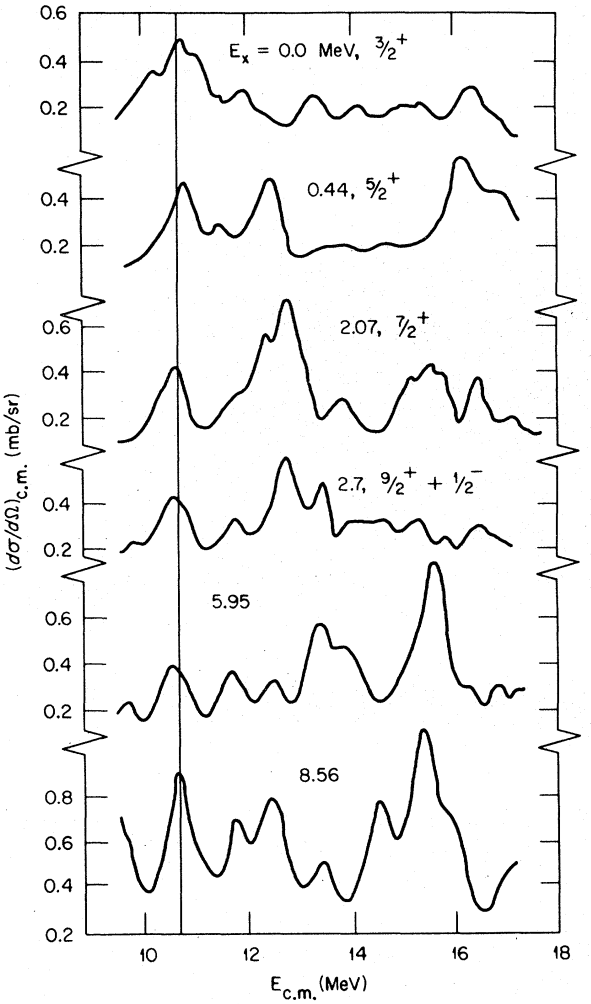

FIG. 7. Some of the $^{12}C(^{15}N,\alpha)$ excitation functions displaying correlated structures near 10.7 MeV (c.m.).

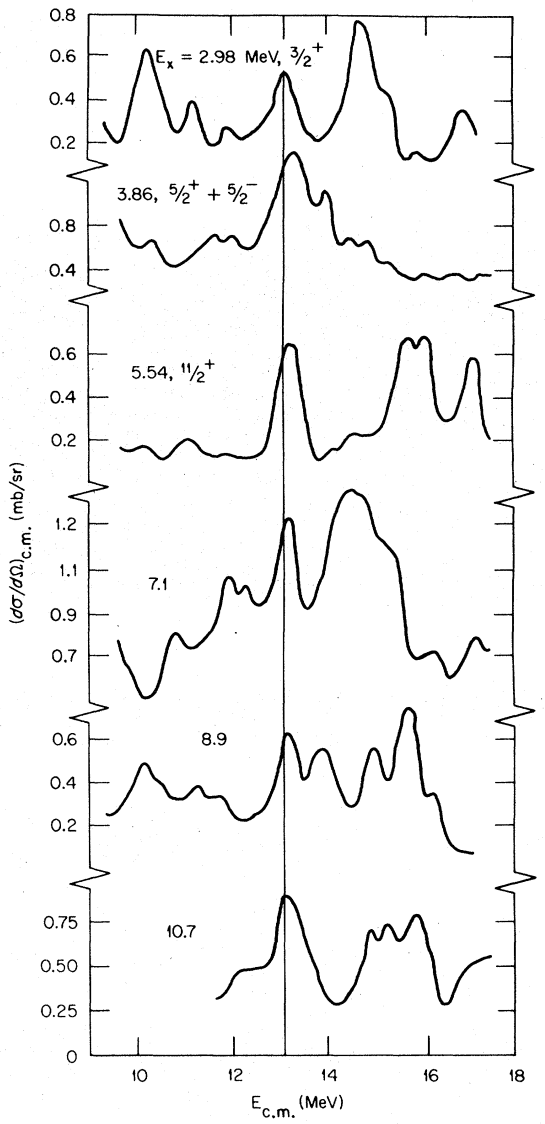

FIG. 8. Some of the $^{12}C(^{15}N,\alpha)$ excitation functions displaying correlated structures near 13.2 MeV (c.m.).

3. *Single-level analysis*

The energy averaged cross sections then contain 216 identified peaks whose widths, magnitudes, and degrees of correlation are all large. Although these features may partially result from statistical processes, the number and strength of the observed structures indicate the presence of strong non-statistical processes in the data. The widths, areas, and centroids of these peaks were analyzed after first subtracting a smooth background passing through the minima of the resonant-like structure. The average width was 0.44 ± 0.1 MeV. The resonant energies of apparently correlated states were averaged to obtain values for the average resonant energy $\overline{E}$ and the standard deviation Δ, which was typically 0.1 MeV. Figure 10(a) displays the number of such α-particle groups as histograms whose positions and widths correspond to $\overline{E} \pm \Delta$ (also see Table II). Some correlation may, of course, be purely statistical in origin. However, the observed structure shows large widths and large deviations from the average cross sections as well as correlated maxima, and these three features of the data appear unlikely to be due to statistical fluctuations alone.

Angular momentum considerations may account for the origin of the resonant structure. When the compound nucleus ^{27}Al is formed at an excitation energy of 32.8 MeV the value of J_c is $\frac{23}{2}$. An extrapolation from the known low-lying yrast states according to the relation $E_J \propto J(J+1)$ yields a value of $\frac{27}{2}$ for the yrast state near this excitation energy if a constant moment of inertia is assumed.

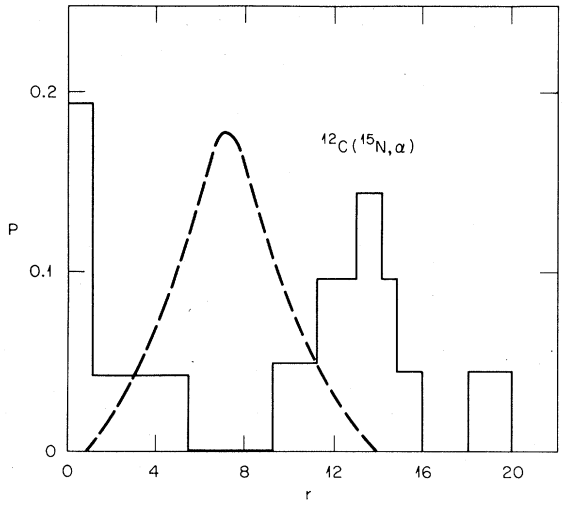

FIG. 9. A histogram showing experimental frequency of observing r maxima in $N=41$ excitation functions for the $^{12}C(^{15}N,\alpha)$ reaction. Also shown is the predicted distribution for observing correlated peaks in statistically fluctuating data as calculated from the binomial distribution.

Actually, this value represents a lower limit since the moment of inertia has been shown to increase for the neighboring nuclei ^{26}Al (Ref. 53) and ^{28}Si (Ref. 54). Therefore, in the present experiment we are in the vicinity of, or approaching the members of the yrast line at high excitation energies in ^{27}Al. This fact is illustrated in Fig. 11 in which are

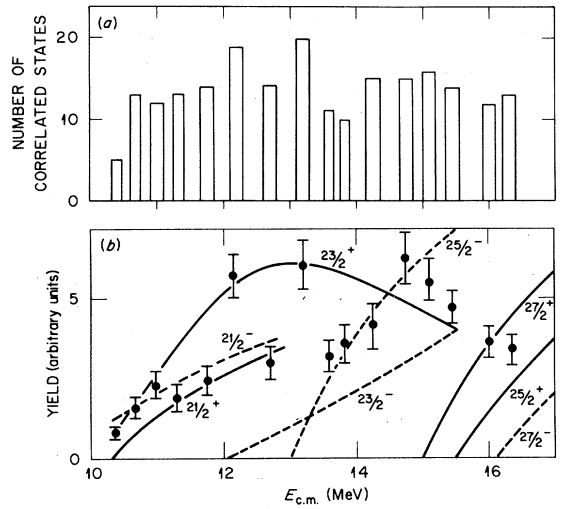

FIG. 10. (a) A histogram indicating the number of correlated states observed as a function of the incident energy (c.m.). See text for further explanation. (b) The sum of the yields, or resonance strengths, for the correlated resonances of (a). Solid and dashed lines are calculated theoretical resonance yields for the spins and parities indicated.

TABLE II. Summary of correlated structures observed in the $^{12}C(^{15}N,\alpha)$ reaction.

E_{in}(c.m.)	E_x (^{27}Al)	Number of correlated states
10.43	27.73	5
10.68	27.97	13
11.00	28.29	12
11.32	28.62	13
11.71	29.00	14
12.19	29.49	19
12.71	30.00	12
13.19	30.49	20
13.61	30.91	11
13.88	31.17	10
14.26	31.56	15
14.76	32.06	15
15.12	32.42	16
15.47	32.77	14
15.97	33.26	12
16.32	33.62	13

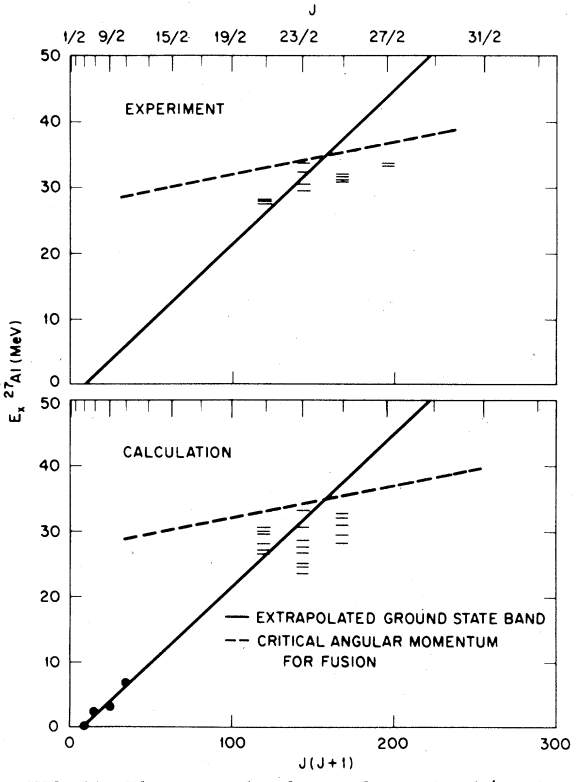

FIG. 11. The extrapolated ground state band (solid line) and Hauser-Feshbach critical angular momenta (dotted line) for the $^{12}C+^{15}N$ system. The short horizontal lines in the top figure are the lowest energy $\frac{21}{2}$, $\frac{23}{2}$, $\frac{25}{2}$, and $\frac{27}{2}$ states suggested from the experimental data by the curves in Fig. 10(b). The states shown in the bottom figure are the lowest energy positive parity $\frac{21}{2}$, $\frac{23}{2}$, and $\frac{25}{2}$ levels according to shell-model calculations (Ref. 21).

plotted angular momenta relevant to the present experiment. The ground state rotational band of ^{27}Al is shown extrapolated from the few members identified at low energies up to high excitation energies. The spin cutoff values J_c determined from the $^{12}C + ^{15}N$ fusion measurements of Kovar *et al.*[42] are also displayed.

Shell-model calculations for *sd* shell nuclei using large shell-model codes such as those performed by McGrory and Wildenthal[55] have successfully described high-spin states in these nuclei.[22,41,56,57] Calculations[21] have recently been made for the case of the ^{27}Al nucleus including positive parity states with spins up to $\frac{27}{2}$ (the maximum spin allowed using the full *sd* shell basis). Results of these calculations are shown in Table III. The calculated average level spacings for spins $\frac{21}{2}^+$, $\frac{23}{2}^+$, $\frac{25}{2}^+$, and $\frac{27}{2}^+$ are then 0.80, 0.93, 1.13, and 3.15 MeV, respectively, and range from two ($\frac{27}{2}^+$) to ten ($\frac{21}{2}^+$) times larger than values predicted by the statistical model.

Comparison of the curves in Fig. 11, along with the shell-model states shown in the botton half of the figure (calculation), indicate that the angular momentum cutoffs used in the Hauser-Feshbach calculations are close to the spin limitation imposed by the yrast line in ^{27}Al. The number of available states in the compound nucleus with spin values close to those of the yrast line are limited. Furthermore, the number of available exit channels also diminishes, as seen in Fig. 12 by comparing the number of open channels given by the quantity $G(J)$ [Eq. (3)] for $J_c \geq \frac{21}{2}$ with those available near the maximum of the curve. Since[58,59]

$$\frac{\Gamma_J}{D_J} \cong \frac{G(J)}{2\pi} , \tag{5}$$

the values of Γ/D obtained from Fig. 12 decrease from around 120 for $J = \frac{21}{2}$ down to two for $J = \frac{29}{2}$. As one condition for the validity of the statistical model requires that $\Gamma/D \gg 1$, it is clear that the applicability of this model for J values greater than about $\frac{21}{2}$ for the $^{12}C(^{15}N,\alpha)$ reaction is dubious. The bumps or "resonances" observed in the $^{12}C(^{15}N,\alpha)$ excitation functions may well then represent a breakdown in the assumption of strongly overlapping levels in the compound nucleus.

In this picture each resonance is due to the excitation of a single or at most a few isolated compound nuclear levels. The resonance strengths may then yield information concerning the compound nuclear spins involved as demonstrated by analyses of (α,p) and (α,n) reactions (see, for example, Refs. 60 and 61). The cross section was approximated by a single-level Breit-Wigner term in which the partial widths were replaced by readily calculable optical-model penetrabilities. Analyses of α particle induced excitation functions with this approximation[60,61] resulted in theoretical curves which form distinct bands for each individual J value, as do the measurements also (based on excitation functions for known spin states). It might be expected that the calculated curve for each J value would need to be independently normalized to the measurements for states of that spin in order to account for the fact that the data were taken on resonance while the Hauser-Feshbach penetrabilities correspond to average cross sections. However, the entire set of calculations for all J values could be reasonably well adjusted to the data by using a single normalization factor.[60,61] Consequently, the different energy dependencies of the bands could be used to suggest the value of the compound nucleus spin involved.

A similar analysis of the $^{12}C(^{15}N,\alpha)$ data in Fig. 10(b) shows the resonant areas as a function of the c.m. energy. The areas of all the peaks correlated at each energy have been summed, after first subtracting the nonresonant background, in order to obtain a measure of the total strength of each resonance. The solid and dashed curves in Fig. 10(b) correspond to calculations for positive and negative parity states. However, it is necessary to normalize the set of calculated curves to the data at one point. Only a narrow range of spin values can contribute to the observed resonant structure. Spins less than J_c will be included in the Hauser-Feshbach calculations and the contri-

TABLE III. Shell-model calculations of the lowest $\frac{21}{2}^+ - \frac{27}{2}^+$ states in ^{27}Al (Ref. 21).

$2J^+$	$E_x(^{27}Al)$							
21	26.65,	27.33,	28.21,	29.63,	30.14,	30.65		
23	23.59,	24.18,	25.17,	26.88,	27.73,	28.22,	30.78,	33.34
25	28.39,	29.60,	31.03,	32.20,	32.94			
27	33.69,	36.84						

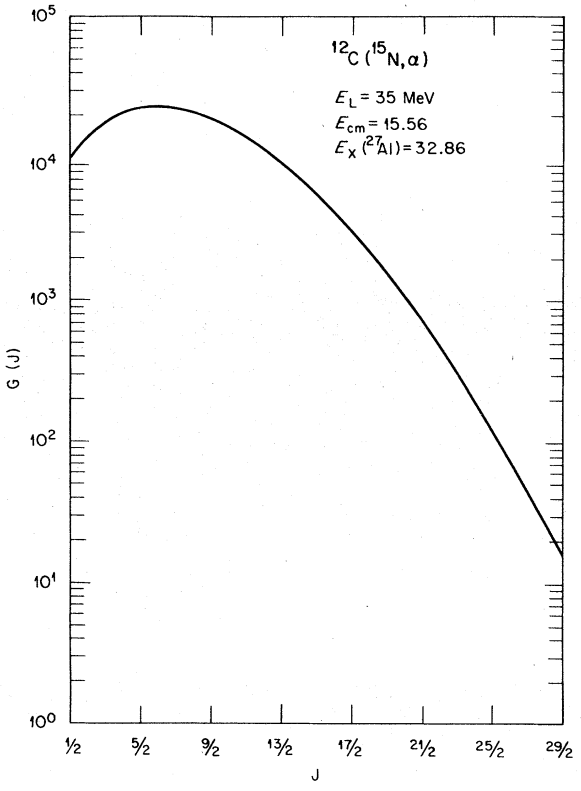

FIG. 12. The Hauser-Feshbach denominator $G(J)$ equal to the number of open channels for the decay of the compound nucleus ^{27}Al at 32.86 MeV into different spins J.

bution of levels with these angular momentum values will be in the general background underlying the resonances. If the total angular momentum is greater than $\frac{27}{2}$, then the transmission coefficients are vanishingly small. Consequently, only spin values between $\frac{21}{2}$ and $\frac{27}{2}$ can produce resonances, since these levels are close to the yrast line and therefore have widths comparable to or less than the level spacing; an argument supported by the shell-model calculations (see Table III). Only normalizing the curve for spin $\frac{23}{2}^+$ to the second resonance at 10.7 MeV provides the satisfactory fit to all the data seen in Fig. 10(b). Note that the curve for each J value terminates at the excitation energy at which $J = J_c$, since for higher energies overlapping resonances are to be expected.

Therefore, the observed $^{12}C(^{15}N,\alpha)$ resonances appear associated with a limited range of high-spin values near the yrast line of ^{27}Al. If the resonances at incident energies of 10.4 and 16.0 MeV (c.m.) are interpreted as due to $\frac{23}{2}^+$ and $\frac{27}{2}^+$ levels, then the excitation energies of these states, 27.6 and 33.2 MeV, respectively, are close to those predicted by an extrapolation of the ground state band. Although the curves in Fig. 10(b) suggest a value for the spin of the level in ^{27}Al corresponding to each observed bump, these values merely indicate the approximate magnitude of the spin involved. Difficulties in locating all the resonant strength, which is spread over many exit channels, in the background subtraction, in the use of data measured at a single angle rather than the integrated cross section, in the use of transmission coefficients rather than partial widths, and in choosing the proper optical-model parameters all contribute to the uncertainty in the spin value. However, the spin values suggested in Fig. 10(b) are indicated in Fig. 11 (top, experimental) where short horizontal lines locate the lowest $\frac{23}{2}$, $\frac{25}{2}$, and $\frac{27}{2}$ levels proposed by this analysis. The experimental and calculated states shown in Fig. 11 are in reasonable agreement.

B. Angular distributions

The angular distribution shown in Fig. 3 displayed strong forward peaking on resonance. Indeed this forward peaking is a significant feature of the angular distribution of an isolated high-spin state in the compound nucleus and is a signature of the excitation of such a high-spin state. In Fig. 13 are calculated angular distributions for a single compound nuclear level of the spin and parity shown. The curves are symmetric about 90°. In these calculations the level widths involved were again approximated by the appropriate optical-model transmission coefficients. Clearly, the higher the spin the more forward peaked is the angular distribution, and thus it is at forward angles that resonant effects such as those observed here will most likely be identified. At more backward angles it becomes more and more likely that the single-level contribution is lost in the sea of Hauser-Feshbach contributions due to the lower spin states in the compound nucleus.

The angular distributions were analyzed by the program PAZIT developed to extract resonant spins from systems where some of the spins may not be zero.[62] This program using the formalism of Lustig[63] assumes that the cross section consists of a resonance term, a background term, and a term describing the interference between these two. The resonance contribution can arise from a single level, many states of the same spin and parity,[63] or a doorway state weakly coupled to the compound nucleus.[64] In addition, the background term may be replaced by a second resonance term so that the cross section due to two states of different spin and/or parity may be computed.

Figure 14 displays angular distributions measured on and off the resonances shown in the inserts of the figure which occur in the excitation functions of the 0.44 and 4.78 MeV levels of ^{23}Na.

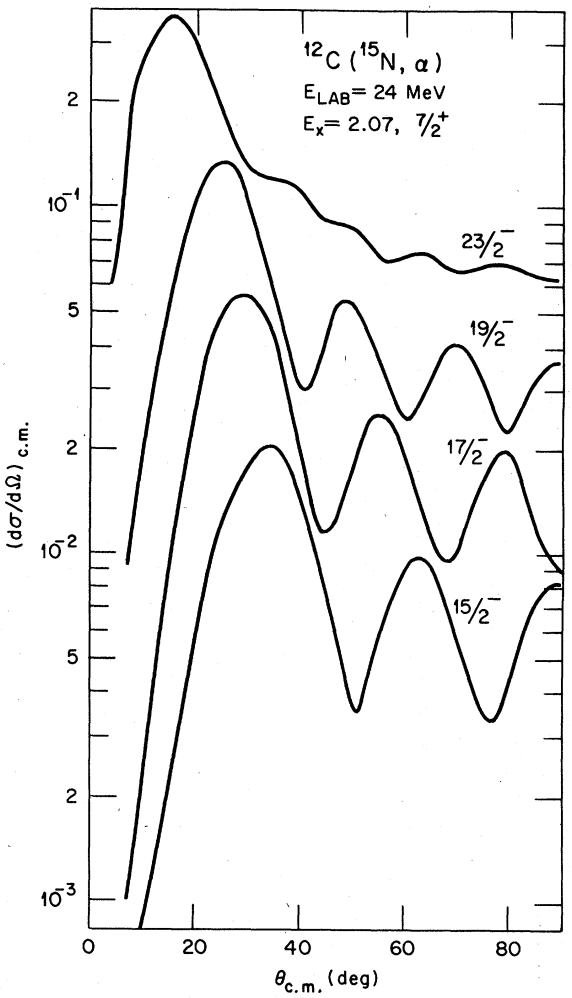

FIG. 13. Angular distributions for isolated compound nucleus levels of various spins calculated with a single-level approximation. The state in the residual nucleus was assumed to be the 2.07-MeV $\frac{7}{2}^+$ level in ^{23}Na.

The strongly forward-rising, on-resonance, angular distributions are reasonably well fitted, assuming compound nuclear spins J_{CN} of $\frac{25}{2}$. These fits are insensitive to the parity of the compound nuclear state, as an arbitrary normalization was used in order to obtain the minimum χ^2 value in the fitting procedure, since in this case positive and negative parity states whose spin values differ by one unit of $\hbar$ will give similar results. This fact is illustrated in Fig. 15, where the χ^2 values for even and odd parity values are given by the solid and dashed lines, respectively. However, a given spin value produces very different angular distribution shapes at forward angles for plus and minus choices of the parity.

The significant feature in Fig. 15 is that the curves have deep minima clearly favoring a

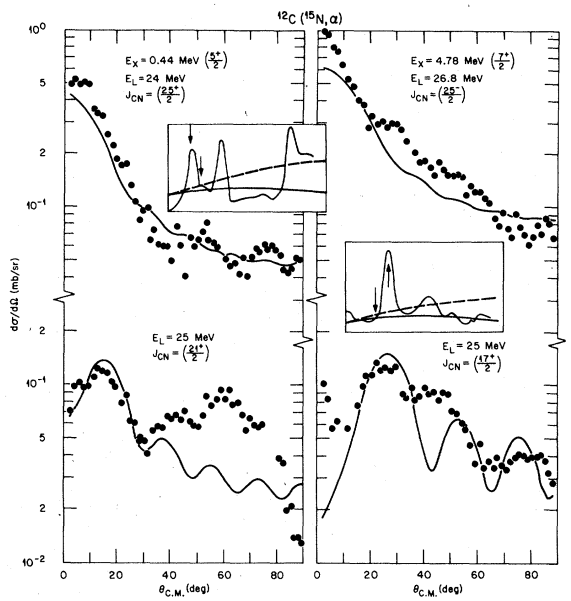

FIG. 14. Comparison of measured angular distributions with single-level calculations on and off the resonant-like structures observed in the excitation functions at 7° for the 0.44-MeV $(\frac{5^+}{2})$ and 4.78-MeV $(\frac{7^+}{2})$ states in ^{23}Na.

limited range of high-spin values. In contrast to the situation on resonance, the off-resonant angular distributions are not well fitted, although the most forward angle portion of the data indicates a J_{CN} value which is definitely lower than the value on resonance. Furthermore, the χ^2 plots, while favoring lower J_{CN} values, have a broad rather than a sharp minimum representative of the poorer fits seen in Fig. 14.

The difficulty in fitting the angular distributions, particularly off resonance, is due in large part to the background contribution to the cross section. As seen in Fig. 13, except at the most forward (and backward) angles, the resonant contribution

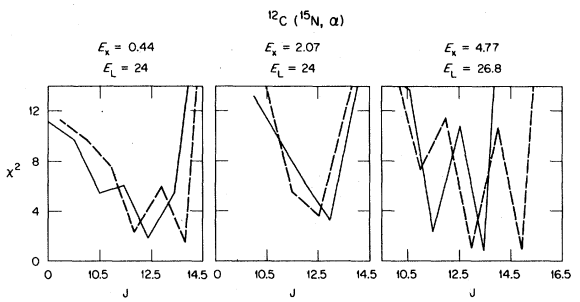

FIG. 15. Sample χ^2 plots for single-level fits at resonant energies. The solid and dashed lines are for positive and negative parity, respectively. These plots are for the angular distributions shown in Figs. 14 and 16.

of a high-spin state will not dominate those due to the large number of low-spin states also present. Describing the background by a Hauser-Feshbach term can only be an approximation, since the angular distributions are not averaged over a range of incident energies. The form of the interference term also presents a problem.

Furthermore, the cross section probably often results not just from a single high-spin state whose contribution is more accurately described by a resonance term rather than the statistical model, but from states with a range of spin values whose contributions cannot be accounted for by a Hauser-Feshbach treatment. To illustrate this point, Fig. 16 shows the angular distribution measured on one of the bumps observed in the 7° (lab) excitation function of the 2.07 MeV ($\frac{7}{2}^+$) state in ^{23}Na. In the upper half of the figure it is seen that the most forward maximum in the angular distribution requires a $J_{CN} = \frac{25}{2}^+$ contribution for a fit. The oscillatory structure appearing at more backward angles is best fitted with the $J_{CN} = \frac{15}{2}^+$ contribution shown in the second half of the figure. Including both the $\frac{25}{2}^+$ and $\frac{15}{2}^+$ terms together with interference between them yields the calculated curve appearing in Fig. 17. Clearly, interference effects are important in fitting these data, and the possibility of having several resonant-like terms as well as a statistical contribution make it unlikely that detailed fits can generally be obtained.

It appears significant, however, that the shape of the angular distributions on resonance indicate that one or a few high-spin states in the compound nucleus are being excited. As the energy is increased from off resonance to on, and then further, to off resonance again, the value of the angular momentum required in order to obtain an acceptable fit to the forward angle data must first increase and then decrease by at least several units of angular momentum. This is yet a fourth feature of the data (see Sec. III A), which is not compatible with present statistical theories.

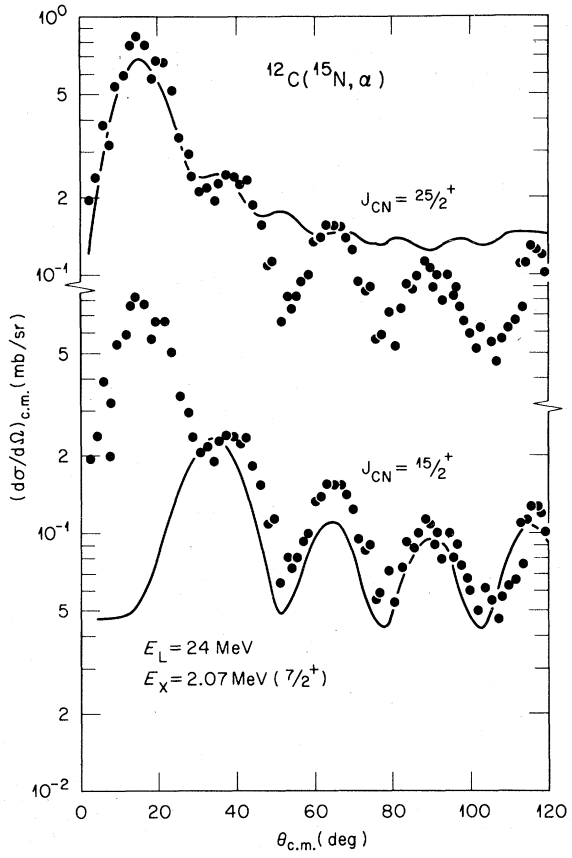

FIG. 16. Single-level calculations for spins of $\frac{25}{2}^+$ and $\frac{15}{2}^+$ which, respectively, provide the best fits for the forward angle and more backward structures in the angular distribution measured at the maxima of the peak observed at 24 MeV in the excitation function for the 2.07-MeV level of ^{23}Na.

C. Elastic scattering data

The ^{12}C(^{15}N, α) angular distributions as well as elastic scattering measurements of light nuclei[30] imply that further support for the presence of resonant effects in the ^{12}C + ^{15}N system might be found from observing backward angle scattering of ^{15}N from ^{12}C. Excitation functions were measured

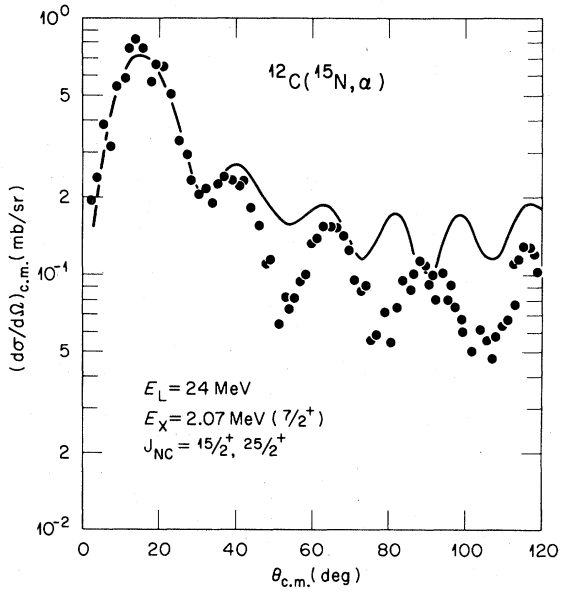

FIG. 17. The data of Fig. 16 fitted with the curve due to resonant and interference terms from two compound nuclear states with spins of $\frac{15}{2}^+$ and $\frac{25}{2}^+$.

at five angles, $160.2° \leq \theta_{c.m.} \leq 169.8°$, spaced at 1.2° intervals. In Fig. 18 the excitation function resulting from an integration over these five angles is plotted. More complete angular distributions measured between 140° and 170° (c.m.) at selected energies appear in Fig. 19.

The excitation function is not featureless, but displays pronounced structure. However, except for the peak at 29.4 MeV (lab) the maxima do not appear to be correlated with the anomolies observed in the α-particle data. Although the angular distributions become more structured as the incident energy is raised, this probably merely reflects the increase in the grazing angular momentum. Thus, the elastic scattering does not generally collaborate the structure observed in the reaction data. The peak at 29.4 MeV (13.06 MeV c.m.), which may be identical to that seen in many of the final state excitation functions from the $^{12}C(^{15}N,\alpha)$ reaction (see Figs. 8 and 10) indicate that some correlations may exist, however, particularly at the higher energies where the scattering described in the optical model diminishes. The grazing angular momenta, and the total angular momenta at which the Hauser-Feshbach cross sections have their maximum values, are sufficiently equal for the elastic and α-particle channels that spin cutoff factors or other angular momentum considerations cannot account for the difference in the behavior of these two channels. It therefore appears that the resonant effects suggested by the reaction data are not due to entrance channel effects.

However, the resonant effects observed in the elastic scattering of light nuclei have been described in terms of surface transparent optical models at both forward and backward angles.[65-69] On the other hand, the nonstatistical effects in the present reaction data have been attributed to the population of states near the yrast line in the compound nucleus. The elastic cross sections predicted by the Hauser-Feshbach calculations in the angular range of Fig. 18, although comparable, are lower than the measured data. Therefore, even at these backward angles, shape elastic scattering may still be dominanting the compound elastic scattering and so masking resonance effects similar to those observed in the reaction data.

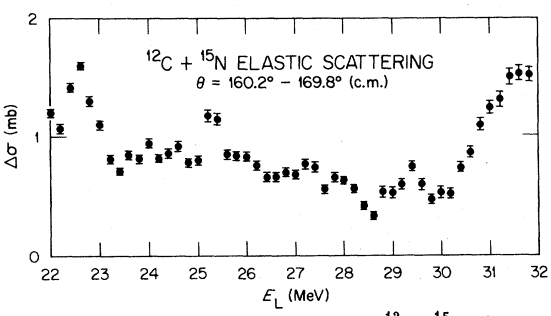

FIG. 18. The excitation function for $^{12}C+^{15}N$ elastic scattering averaged over the angular interval 160.2° to 169.8° (c.m.).

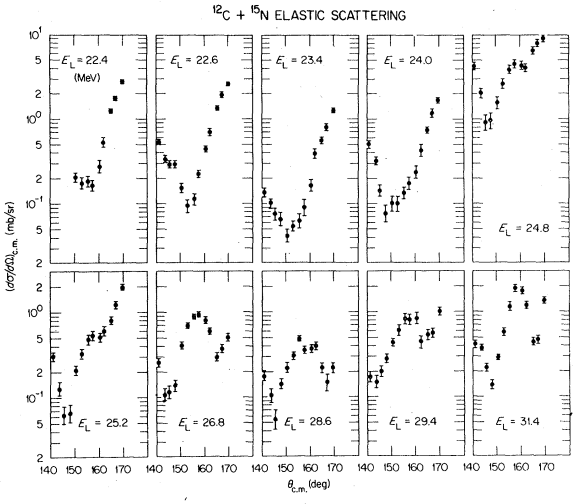

FIG. 19. Angular distributions for $^{12}C+^{15}N$ elastic scattering measured at backward angles.

IV. DISCUSSION

The usual criteria for the existance of resonances or intermediate structure in reactions require: (1) deviations from the average cross sections larger than expected by the statistical model and (2) correlations between the structures observed in the excitation functions for different final states, exit channels, and reaction angles. The size of the structure seen in the $^{12}C(^{15}N,\alpha)$ reaction seems outside the limit expected from a statistical reaction mechanism. Although detailed excitation functions were only measured at 7° (lab), the angular distributions indicate that excitation functions measured at various angles will generally also display the anomalies seen in the excitation function at 7°. However, if these anomolies are due to relatively isolated high-spin states in the compound nucleus, then, as suggested by Fig. 13, the single-level contribution becomes increasingly harder to identify as the reaction angle is increased. The existence of structure in the $^{12}C+^{15}N$ neutron channels has been investigated by measuring the total emitted neutron yield with the ORNL 4π graphite sphere detector.[70] Although the yield curve is smooth and displays no resonant effects, such a measurement places a severe condition on the observation of resonances since all

neutron emitting processes, all final states, and all angles are included. As pointed out by Feshbach,[71] the variation in partial widths for different exit channels may prevent a resonance from being seen in some channels. However, the structure in the α channel should appear in the elastic scattering if the resonances are due to entrance channel effects. Failure of correlated structure to be present makes the interpretation of the $^{12}C(^{15}N, \alpha)$ data more difficult. Nevertheless, the explanation of the α-particle anomalies as originating from the population of high-spin states near the yrast line of the compound nucleus is compatible with the present data although the Hauser-Feshbach calculations are not significantly lower than the backward angle elastic scattering. Coulomb and shape elastic scattering will tend to mask structure from this proposed mechanism in the elastic scattering at more forward angles.

The location of the yrast line in ^{27}Al clearly is important in understanding the present data. Recently the determination of level densities and the position of the yrast line in *sd* shell nuclei have received attention since they affect the nature and location of quasimolecular states and resonances[72,73] and the understanding of angular momentum limitations imposed on fusion cross sections.[74-76] Calculated yrast lines using the Strutinsky method and including pairing corrections for nuclei in the mass region of ^{27}Al indicate that the yrast states with spins between 10 and 16 $\hbar$ occur for excitation energies between about 20 and 35 MeV.[74,75] The shell-model results of McGrory[21] are in agreement with these calculations. In addition, Lee *et al.*[76] suggest that the limitation on light heavy ion fusion cross sections can be understood in terms of a "statistical yrast line," approximately 10 MeV higher than the actual yrast line, and which determines the level in the compound nucleus in which the level density is sufficiently high that fusion can occur. These points indicate that the position of the levels shown in Fig. 11 are at excitation energies where the level density is low enough so that the applicability of the statistical model is suspect.

However, it is possible that the low density of high-spin states in the compound nucleus excitation energy region populated in the present experiment may not simply require that the excitation of these states be described by a single-level or R-matrix-like approach. The low density may cause an increase in different fluctuation phenomena. For circumstances where the number of open channels is small, Moldauer has shown that fluctuations can produce widths which may be several times as large as the coherence width.[77] But the angular momentum features observed in the $^{12}C + ^{15}N$ system are not explained in this picture. Of course, the Hauser-Feshbach formalism, the number of open channels, and the compound partial widths which determine the coherence width obtained from analyzing the fluctuations in excitation functions all depend strongly on the total angular momentum J involved.[26] However, in deciding whether or not a set of excitation function data can be described by the statistical model, the number and magnitude of observed peaks must also be compared with expected values. The usual probability functions used to analyze the number of peaks in an excitation function, Eq. (4), and the distribution of cross section values about the average value [Eq. (1) of Ref. 41], are largely insensitive to the spin values J in the compound nucleus. Although the distribution of cross section values involves N_{eff}, the number of effective channels participating in the reaction, which in turn depends upon a summation over angular momenta including J[16]; N_{eff} depends most sensitively on the spins in the entrance and exit channels. Furthermore, it is difficult to determine parameters such as N_{eff} from fitting experimental probability distributions.[41] As a result, it is not easy to test the dependence of measured cross section distributions on the spin values which may be populated in the compound nucleus. The low density of high-spin states populated in the present experiment may cause fluctuations in the number or spin of high-spin states excited about the average distribution predicted by the statistical model. Thus a more general fluctuation picture may encompass the present data.

The forward peaked angular distributions are also compatible with direct reactions. But such a reaction mechanism does not seem capable of describing either the resonant-like peaks observed or the high angular momentum effects indicated by the excitation functions and angular distributions. Massive transfer such as of ^{11}B nuclei also seems improbable at these energies.

V. CONCLUSIONS

Analysis of the excitation functions of the $^{12}C(^{15}N, \alpha)$ reaction at a laboratory angle of 7° indicate the presence of a large number of anomalies that fall outside statistical model predictions. These anomalies manifest themselves as large fluctuations (resonances) with widths of two or three times the coherence width and with an unusually large number of correlations among the α groups studied. An explanation for the observed resonances based on the resonant strengths in the excitation functions appears to be the population of high-spin states close or at the yrast line

of the compound nucleus ^{27}Al.

Angular distributions measured at selected energies between 2° and 110° (c.m.) have been compared with single-level calculations. These calculations, assuming the excitation of high-spin states in the compound nucleus, reproduce the strong forward peaking of the angular distributions measured on resonance. Furthermore, the angular distributions favor higher compound nuclear spins on resonance than at nonresonant energies.

The elastic scattering excitation functions at backward angles display structure as well, but this structure is not well correlated to that observed in the α-particle channels. Therefore, the anomalies in the reaction data do not appear to be an entrance channel phenomena.

These data are generally understandable as arising from high angular momentum states for which the number of open channels is small, and hence for J values which should not be included in Hauser-Feshbach calculations. Thus, these anomalies appear to be due to relatively isolated levels resonanting, in contrast to mechanisms such as shape or molecular resonances used to interpret many heavy ion scattering and reaction data. However, the growing profusion of resonances being reported for heavy ion systems suggest that effects similar to those discussed here should be kept in mind.

ACKNOWLEDGMENTS

This research was sponsored in part by the Division of High Energy and Nuclear Physics, Office of Energy Research, U. S. Dept. of Energy, under Contract No. W-7405-eng-26 with Union Carbide Corporation, and by CONACYT (Contract PNCB-0022), Mexico.

[1]E. Vogt, *Advances in Nuclear Physics*, edited by M. Baranger and E. Vogt (Plenum, New York, 1968), p. 261.

[2]M. Bohning, *Nuclear Reactions Induced by Heavy Ions*, edited by R. Bock and W. R. Hering (North-Holland, Amsterdam, 1970), p. 633.

[3]R. G. Stokstad, *Proceedings of the International Conference on Reactions between Complex Nuclei, Nashville, Tennessee, 1974*, edited by R. L. Robinson, F. K. McGowan, J. B. Ball, and J. H. Hamilton (North-Holland, Amsterdam, 1974), p. 327.

[4]H. V. Klapdor, in *Proceedings of the International Conference on Nuclear Interactions, Canberra, Australia*, edited by B. A. Robson (Springer, Heidelberg, 1979), p. 125.

[5]J. Gomez del Campo, M. E. Ortiz, A. Dacal, J. L. C. Ford, Jr., R. L. Robinson, P. H. Stelson, and S. T. Thornton, Nucl. Phys. A262, 125 (1976).

[6]See, for example, the papers in *Nuclear Molecular Phenomena*, edited by N. Cindro (North-Holland, Amsterdam, 1978).

[7]R. Middleton, J. D. Garrett, and H. T. Fortune, Phys. Rev. Lett. 27, 950 (1971).

[8]L. R. Greenwood, R. E. Segel, K. Raghunathan, M. A. Lee, H. T. Fortune, and J. R. Erskine, Phys. Rev. C 12, 156 (1975).

[9]D. Fick, see Ref. 6, p. 269.

[10]J. L. 'Ecuyer, R. Volders, C. Cardinal, L. Deschênes, and N. Marquardt, Phys. Rev. C 12, 1878 (1975).

[11]N. Marquardt, W. Hoppe, and D. Siegel, Phys. Rev. C 16, 2291 (1977).

[12]J. F. Mateja, A. D. Frawley, A. Roy, J. R. Hurd, and N. R. Fletcher, Phys. Rev. C 18, 2622 (1978).

[13]L. C. Dennis, K. R. Cordell, R. R. Doering, S. T. Thornton, R. L. Parks, J. L. C. Ford, Jr., J. Gomez del Campo, and D. Shapira (unpublished).

[14]A. D. Frawley, J. F. Mateja, A. Roy, and N. R. Fletcher, Phys. Rev. C 19, 2215 (1979).

[15]D. J. Crozier and J. C. Legg, Phys. Rev. Lett. 33, 782 (1974).

[16]R. A. Dayras, R. G. Stokstad, Z. E. Switkowski, and R. M. Wieland, Nucl. Phys. A265, 153 (1976).

[17]K. R. Cordell, S. T. Thornton, L. C. Dennis, P. G. Lookadoo, T. C. Schweizer, J. L. C. Ford, Jr., J. Gomez del Campo, and D. Shapira, Nucl. Phys. A323, 147 (1979).

[18]K. R. Cordell, S. T. Thornton, L. C. Dennis, T. C. Schweizer, J. Gomez del Campo, and J. L. C. Ford, Jr., Nucl. Phys. A296, 278 (1978).

[19]J. Gomez del Campo, J. L. C. Ford, Jr., R. L. Robinson, M. E. Ortiz, A. Dacal, and E. Andrade, Phys. Lett. 69B, 415 (1977).

[20]H. T. Fortune, R. R. Betts, and R. Middleton, Phys. Rev. C 16, 401 (1978).

[21]J. B. McGrory, private communication.

[22]J. Gomez del Campo, D. E. Gustafson, R. L. Robinson, P. H. Stelson, P. D. Miller, J. K. Bair, and J. B. McGrory, Phys. Rev. C 12, 1247 (1975).

[23]G. J. Kekelis, A. H. Lumpkin, K. W. Kemper, and J. D. Fox, Phys. Rev. C 15, 664 (1977).

[24]C. E. Moss, Nucl. Phys. A269, 429 (1976).

[25]P. M. Endt and C. Van der Leun, Nucl. Phys. A310, 1 (1978).

[26]J. Gomez del Campo, J. L. C. Ford, Jr., R. L. Robinson, M. E. Ortiz, A. Dacal, and E. Andrade, Nucl. Phys. A297, 125 (1978).

[27]D. Shapira, R. G. Stokstad, and D. A. Bromley, Phys. Rev. C 10, 1063 (1974).

[28]D. E. Gustafson, S. T. Thornton, T. C. Schweizer, J. L. C. Ford, Jr., P. D. Miller, R. L. Robinson, and P. H. Stelson, Phys. Rev. C 13, 691 (1976).

[29]S. T. Thornton, D. E. Gustafson, K. R. Cordell, L. C. Dennis, T. C. Schweizer, and J. L. C. Ford, Jr., Phys. Rev. C 17, 576 (1978).

[30]See, for example, *Proceedings of the Symposium on Heavy-Ion Elastic Scattering*, edited by R. M. DeVries

(University of Rochester, Rochester, 1977).
[31]D. Shapira, G. L. Bomar, J. L. C. Ford, Jr., J. Gomez del Campo, and L. C. Dennis, Nucl. Instrum. Methods 169, 77 (1980).
[32]M. G. Braga Marcazzan and L. Milazzo Colli, *Progress of Nuclear Physics*, edited by D. M. Brink and J. H. Mulvey (Pergamon, Oxford, 1970), Vol. II, p. 145.
[33]A. Richter, *Nuclear Spectroscopy and Reactions*, edited by J. Cerny (Academic, New York, 1974), p. 343.
[34]M. L. Halbert, F. E. Durham, and A. van der Woude, Phys. Rev. 162, 899 (1967); M. L. Halbert, F. E. Durham, C. D. Moak, and A. Zucker, *ibid.* 162, 919 (1967).
[35]H. T. King, M. Hass, G. Glashausser, M. Sosnowski, and A. B. Robbins, Nucl. Phys. A322, 159 (1979).
[36]L. R. Greenwood, K. Katori, R. E. Malmin, T. H. Braid, J. C. Stoltzfus, and R. H. Siemssen, Phys. Rev. C 6, 2112 (1972).
[37]J. L. C. Ford, Jr., J. Gomez del Campo, R. L. Robinson, P. H. Stelson, and S. T. Thornton, Nucl. Phys. A226, 189 (1974).
[38]G. Pappalardo, Phys. Lett. 13, 320 (1964).
[39]W. Hauser and H. Feshbach, Phys. Rev. 87, 366 (1952).
[40]S. K. Penny, Oak Ridge National Laboratory (to be published).
[41]J. Gomez del Campo, J. L. C. Ford, Jr., R. L. Robinson, P. H. Stelson, and S. T. Thornton, Phys. Rev. C 9, 1258 (1974).
[42]D. G. Kovar, D. F. Geesaman, T. H. Braid, Y. Eisen, W. Henning, T. R. Ophel, M. Paul, K. E. Rehm, S. J. Sanders, P. Sperr, J. P. Schiffer, S. L. Tabor, S. Vigdor, B. Zeidman, and F. W. Prosser, Jr., Phys. Rev. C 20, 1305 (1979).
[43]V. Facchini and E. Saetta-Menichella, Energ. Nucl. (Milan) 15, 54 (1968).
[44]A. Gilbert and A. G. W. Cameron, Can. J. Phys. 43, 1446 (1965).
[45]J. Lega and P. C. Macq, Nucl. Phys. A218, 429 (1974).
[46]C. M. Perey and F. G. Perey, Nucl. Data B10, 539 (1972).
[47]A. J. Buffa, Jr. and M. K. Brussel, Nucl. Phys. A195, 545 (1972).
[48]R. E. Malmin, Ph.D. thesis, Indiana University, 1972 (unpublished).
[49]W. Reilly, R. Weiland, A. Gobbi, M. W. Sachs, and D. A. Bromley, Nuovo Cimento 13A, 897 (1973).
[50]D. L. Hanson, R. G. Stokstad, K. A. Erb, C. Olmer, and D. A. Bromley, Phys. Rev. C 9, 929 (1974).
[51]C. Volant, M. Conjeaud, S. Harar, S. M. Lee, A. Lepine, and E. F. Da Silveira, Nucl. Phys. A238, 120 (1975).
[52]H. V. Klapdor, G. Rosner, H. Reiss, and M. Schrader, Nucl. Phys. A244, 157 (1975).
[53]J. Gomez del Campo, R. G. Stokstad, J. A. Biggerstaff, R. A. Dayras, A. H. Snell, and P. H. Stelson, Phys. Rev. C 19, 2170 (1979).
[54]M. Conjeaud, S. Gary, S. Harar, and J. P. Wieleczko, Nucl. Phys. A309, 515 (1978).
[55]J. B. McGrory and B. H. Wildenthal, Phys. Rev. C 7, 974 (1973).
[56]B. J. Cole, D. Kelvin, A. Watt, and R. R. Whitehead, J. Phys. G 3, 919 (1977).
[57]J. L. C. Ford, Jr., T. P. Cleary, J. Gomez del Campo, D. C. Hensley, D. Shapira, and K. S. Toth, Phys. Rev. C 21, 764 (1980).
[58]T. Erickson, Ann. Phys. (N.Y.) 23, 390 (1963).
[59]K. A. Eberhard, P. von Brentano, M. Bohning, and R. O. Stephen, Nucl. Phys. A125, 673 (1969).
[60]E. Sheldon, W. A. Schier, G. P. Couchell, B. K. Barnes, D. Donati, J. J. Egan, P. Harihar, S. C. Mathur, and A. Mittler, in *Proceedings of the International Conference on Statistical Properties of Nuclei*, edited by J. B. Garg (Plenum, New York, 1971), p. 121.
[61]W. A. Schier, B. K. Barnes, G. P. Couchell, J. J. Egan, P. Harihar, S. C. Mathur, A. Mittler, and E. Sheldon, Nucl. Phys. A254, 80 (1975).
[62]D. Shapira, R. M. DeVries, M. R. Clover, R. N. Boyd, and R. N. Cherry, Jr., Phys. Lett. 71B, 293 (1977).
[63]H. Lustig, Phys. Rev. 117, 1317 (1960).
[64]D. Robson and A. M. Lane, Phys. Rev. 161, 982 (1967).
[65]A. Gobbi, R. Wieland, L. Chua, D. Shapira, and D. A. Bromley, Phys. Rev. C 7, 30 (1973).
[66]E. H. Auerbach, A. J. Baltz, M. Golin, S. H. Kahana, see Ref. 30, p. 394.
[67]V. Shkolnik, D. Dehnhard, S. Kubono, M. A. Franey, and S. Tripp, Phys. Lett. 74B, 195 (1978).
[68]D. Dehnhard, V. Shkolnik, and M. A. Franey, Phys. Rev. Lett. 40, 1549 (1978).
[69]M. S. Chiou, J. V. Maher, C. M. Cheng, W. Oelert, and W. J. Jordan, Phys. Rev. C 20, 851 (1979).
[70]J. Gomez del Campo, J. K. Bair, and J. L. C. Ford, Jr. (unpublished).
[71]H. Feshbach, J. Phys. (Paris) Colloq. 35 C5-177 (1976).
[72]D. Pocanic and N. Cindro, J. Phys. G 5, L25 (1979).
[73]N. Cindro and D. Pocanic, J. Phys. G 6, 359 (1980).
[74]D. Glas and U. Mosel, Phys. Lett. 78B, 9 (1978).
[75]M. Diebel, D. Glas, U. Mosel, and H. Chandra, Nucl. Phys. A333, 253 (1980).
[76]S. M. Lee, T. Matsuse, and A. Arima (unpublished).
[77]P. A. Moldauer, Phys. Rev. C 11, 426 (1975).